Effect of Polystyrene Latex Addition on Size and Pore Volume of Porous Calcium Oxide Particles Prepared by Spray-Pyrolysis Method and Its Ability for SO_2 Retention

Ricky Dwi Septianto[1], Ferry Iskandar[1,2*], Mikrajuddin Abdullah[1], Khairurrijal Khairurrijal[1] & Myong-Hwa Lee[3]

[1]Physics of Electronic Materials Division, Department of Physics
Faculty of Mathematics and Natural Sciences, Insitut Teknologi Bandung
Jalan Ganesha 10, Bandung 40132, Indonesia
[2]Research Center for Nanosciences and Nanotechnology (RCNN)
Institut Teknologi Bandung, Jalan Ganesha 10, Bandung 40132, Indonesia
[3]Thermochemical Energy System R&D Group, Korea Institute of Industrial Technology (KITECH), 89 Yangdaegiro-gil, Ipjang-myeon, Cheonan, Chungnam 31056, Republic of Korea
*E-mail: ferry@fi.itb.ac.id

Abstract. In this study, the effects of polystyrene (PS) latex addition on the particle morphology and the pore content of calcium oxide (CaO) were investigated. The CaO particles were prepared using an ultrasonic nebulizer-assisted spray-pyrolysis method with variation of the PS/$Ca(NO_3)_2 \cdot 4H_2O$ mass ratio in the precursor. Good crystallinity of CaO was obtained at 825 °C of synthesis temperature under 2 l/min of nitrogen gas flow, which was confirmed by Fourier transform infrared (FTIR) spectroscopy and X-ray diffraction (XRD). According to scanning electron microscope (SEM) characterization, the CaO particles synthesized with 0 and 25 wt% PS addition had an almost spherical shape with an average size of 1.58 and 1.48 μm, respectively. In addition, macropores were formed in the CaO particles prepared with 25 wt% PS addition that had an average pore diameter of 583.26 nm. Meanwhile, the CaO particles prepared with 75 wt% PS addition had a random shape and an average size of 1.41 μm. The mesopore content was investigated by Barret-Joyner-Halenda (BJH) analysis, which showed improvement of the pore size from 3.45 nm to 5.42 nm for 0 and 25 wt% PS addition, respectively, which is proportional to the pore volume, pore surface area, and the capacity of SO_2 retention.

Keywords: *CaO; porous; polystyrene; spray-pyrolysis; SO_2.*

1 Introduction

Recently, the development of flue-gas desulfurization (FGD) materials and systems to support eco-industrial environments has received great attention from industry. Several FGD techniques have been developed involving the development of sorbent materials. Calcium oxide (CaO) and calcium hydroxide ($Ca(OH)_2$) are promising sorbents for capturing hazardous flue gases such as carbon dioxide and sulfur dioxide. Numerous investigations have been

Received July 22nd, 2017, Revised June 4th, 2018, Accepted for publication June 6th, 2018.
 ISSN: 2337-5779, DOI: 10.5614/j.eng.technol.sci.2018.50.2.6

conducted to optimize CaO or $Ca(OH)_2$ performance in reducing SO_2, from investigation of the effect of temperature [1], investigation of the reaction kinetics between CaO and SO_2 [2], the effect of catalyst addition [3], composite formation [4], to the investigation of surface area through the development of fabrication methods such as ethylene glycol (EG)-assisted synthesis [5], sol-gel synthesis [6], thermal decomposition [7], and spray-drying or pyrolysis [8,9].

The adsorption ability of sorbents depends on their active surface to interact with the gas, which is affected by the total surface area, size and volume of the particle pores. Therefore, controlling the particle morphology to reach a high surface area is crucial. A high surface area of the particles can be achieved by reducing the particles to the nanometer scale, resulting in nanoparticles. Fabrication methods that can be used to produce nanometer-sized sorbent particles are thermal decomposition [7] and sol-gel synthesis [10]. However, the use of nanoparticles has some disadvantages, not only related to health and environmental problems but also because of the use of additional materials that make the process more inefficient [11]. Another way to increase the adsorption ability is to modify the shape or morphology of the particles.

Spray-pyrolysis is known as a method that allows the morphology of the particles to be controlled [12]. This is the most facile of the methods mentioned above. By using this method, the particle morphology can be formed to become porous or hollow by way of the addition of easily decomposed materials such as polystyrene (PS) [13-15]. In many cases, porous particles improve photocatalytic performance and have better adsorption properties than dense or non-porous particles [11,15,16].

Furthermore, to the best of our knowledge, little has been published on CaO morphology prepared by PS-assisted spray-pyrolysis and its ability to capture SO_2. Therefore, our aim in this research was to synthesize porous CaO by spray-pyrolysis using PS latex and to investigate the effect of PS addition on the particle morphology, specifically pore content and pore volume.

2 Experimental Method

200-nm PS particles were synthesized by liquid-phase synthesis [13] using styrene monomer and potassium peroxydisulfate (KPS, Merck) as an initiator in distilled water. In brief, firstly styrene monomer was washed in a 2M NaOH solution for 30 min. The mixture was then kept for several minutes to separate the styrene from the NaOH solution; the washed styrene monomer had a transparent-yellowish color. At the same time, distilled water was heated to a temperature of 80 °C and vigorously stirred at 600 rpm in a three-neck reactor. After that, the styrene monomer was added to the heated water, producing a

2-wt% solution of styrene. Then the solution was stirred for 15 minutes to ensure the styrene monomer was evenly spread in the reactor. To start the polymerization reaction, the KPS solution was added to the styrene solution and the process was kept for 10 hours under nitrogen atmosphere.

Figure 1 shows the setup of the spray-pyrolysis system that was used to produce CaO powder. The reactor had three main parts: (i) an ultrasonic nebulizer working at 1.7 MHz as the atomizer that produces precursor droplets with a mean diameter size of 4.47 µm (Figure 1b); (ii) a horizontal tubular furnace with an inner diameter of 3 cm, an electrical heater with a length of 50 cm and two temperature controls; (iii) a bag filter as the powder collector. $Ca(NO_3)_2{\cdot}4H_2O$ (Sigma-Aldrich) was used as raw material to produce the CaO. As precursor, $Ca(NO_3)_2$ was dissolved in distilled water at a concentration of 10 wt%. PS solution was added to the solution with varying the PS/$Ca(NO_3)_2$ mass ratio at 0, 25, and 75 wt%. The precursor was then placed into a nebulizer chamber. Initially, the temperature of the reactor was varied to find the minimum temperature of the reactor that completely converted the $Ca(NO_3)_2$ under a nitrogen atmosphere with a flow rate of 2 l/min.

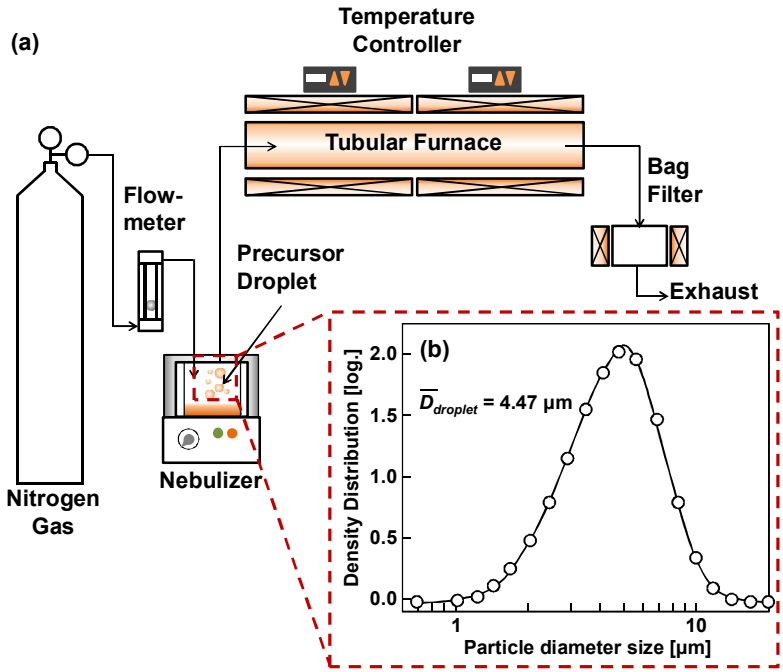

Figure 1 (a) Schematic of spray-pyrolysis system for producing CaO powder and (b) precursor droplet size distribution.

An SO_2 adsorption performance test was conducted to determine the CaO's ability to capture SO_2 gas. A simple test apparatus was built utilizing the solubility of SO_2 in water. The performance test reactor had three main parts: (i) an SO_2 production chamber; (ii) a vertical tube (1 cm inner diameter and 20 cm length) for CaO powder (containing 0.15 g of sorbent and glass beads as powder cantilever) with a belt heater operating at 310 °C on the outer surface of the tube; (iii) a water trap containing 100 ml of water. SO_2 gas was generated by utilizing the reaction between chloride acid (HCl) and sodium sulfite (Na_2SO_3) [17]. 2 M HCl was dropped onto Na_2SO_3 powder with a rate of 1 drop (0.05 ml) per minute in a closed three-neck flask. The formed SO_2 was then flowed to a vertical tube by nitrogen gas flowing at a rate of 0.1 l/min. Finally, the flowed gases were trapped in the water. The pH of the water was evaluated by pH analyzer (HORIBA) every 5 minutes.

The morphology of the sample powder was observed by scanning electron microscopy (SEM, JEOL-JSM-6510LA operated at 10kV). To examine the chemical bonds and elements in the samples, Fourier transform infrared (Omron Bruker Alpha) and energy dispersive X-ray spectroscopy (EDS, JEOL EDS) were used, respectively. X-ray diffractograms (XRD, Bruker D8 Advanced) were used to analyze the crystal structure of the samples. The pore diameter and the pore volume were determined using the Barret-Joyner-Halenda (BJH, Quantachrome BET Autosorb iQ/MP-XR) method. The droplet size and particle size of the samples were measured by particle size analyzer (PSA, HELOS Particle Size Analyzer, RODOS).

3 Result and Discussion

Figure 2(a) shows IR spectra of the samples prepared under various temperatures of the reactor. According to FTIR characterization (Figure 2(a)), the $Ca(NO_3)_2$ was completely decomposed after the temperature reached 825 °C. A sharp peak below 600 cm^{-1} shows the appearance of Ca-O bonding [18,19], while the observed sharp peak around wavenumber 3656 cm^{-1} corresponds to OH groups in the presence of $Ca(OH)_2$[18,20,21]. On the other hand, there are sharp peaks around 1300-1500 cm^{-1} in the samples prepared at 625 °C. These peaks could indicate the nitride bond that also appears in $Ca(NO_3)_2$. The appearance of these peaks shows that the temperature of 625 °C was insufficient to decompose the $Ca(NO_3)_2$, resulting in high impurity of the samples. As the temperature increased to 725 °C, the peak around 1300-1500 cm^{-1} is started to decrease. The high purity of the powder samples prepared at 825 °C was shown by the EDS result (Figure 2(b)). Based on the EDS result, the elements in the sample were Ca (with the highest fraction), O, and C, while N had disappeared. The absence of the N element indicates the complete conversion of $Ca(NO_3)_2$ into the product.

The existence of the C element indicates the formation of $CaCO_3$, which was also observed by FTIR. The presence of two peaks around 878 cm^{-1} and 1444 cm^{-1} in Figure 2(b) and 2(c), is related to the appearance of CO_3^{2-} out-of-plane bending [7,18]. The appearance of $CaCO_3$ may due to a spontaneous reaction of CaO with CO_2 from the environments. However, PS addition did not affect the purity of the CaO samples, as given by FTIR (Figure 2(c)). The FTIR result shows that the CaO samples with low (25%) and high (75%) PS addition, had identical IR spectra compared to the 0% PS addition, which implies that the PS was also completely decomposed. Moreover, the crystal structure of the sample was shown by the XRD that was performed on the samples with high PS addition (75%) (Figure 2(d)). The XRD pattern shows that the formation of multi-phase crystalline was observed, consisting of CaO, $CaCO_3$, and $Ca(OH)_2$ crystals [8,22, 23].

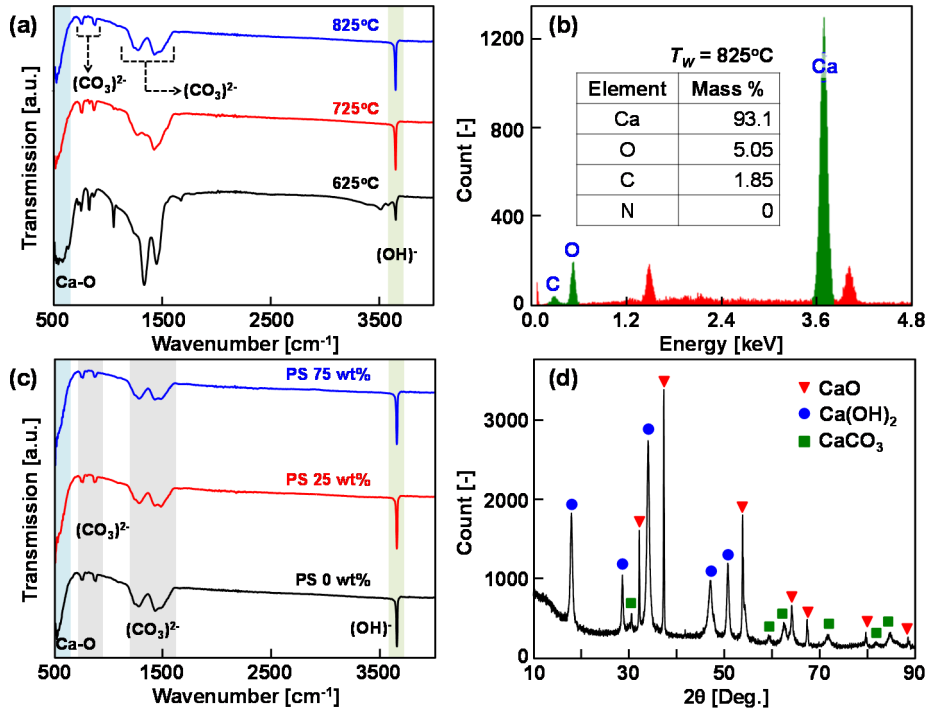

Figure 2 (a) FTIR characterization result of samples prepared at various reactor temperatures, (b) EDS of powder sample prepared at a synthesis temperature of 825 °C, (c) FTIR characterization result of samples prepared with various concentrations of PS in the precursor, and (d) XRD result of powder sample prepared at 825 °C with a PS/$Ca(NO_3)_2$ ratio of 75 wt% in the precursor. CaO, $Ca(OH)_2$, and $CaCO_3$ peaks correspond to PDF File Cards No. 04-005-4757, 00-001-1079, and 04-007-8659, respectively.

The existence of $CaCO_3$ and $Ca(OH)_2$ peaks in the XRD is consistent with the FTIR spectrum that shows the hygroscopic nature of CaO [24] and the capability of CaO to capture CO_2 [8]. Furthermore, the crystal size of the CaO sample was calculated by using Scherrer's equation [25], in Eq. (1) as follows:

$$d_{hkl} = \frac{k\lambda}{\beta \cos\theta} \tag{1}$$

Considering that k = 0.9, λ = 1.54 Å (Cu Kα radiation), and β is full-width at half maximum of the x-ray peak, the crystal sizes (d_{hkl}) of the CaO and the $Ca(OH)_2$ could be determined, which were 48.12 nm (at 2θ = 37.34°) and 14.15 nm (at 2θ = 34.05°), respectively. The crystal size of the CaO, which was larger than that of $Ca(OH)_2$, shows the original formation of CaO followed by the formation of $Ca(OH)_2$ when the as-prepared CaO was exposed to air. The characteristics of this multi-phase crystal were also shown by the CaO with 0% PS addition, thus, the purpose of PS addition as an easily decomposed template material was demonstrated here.

Figure 3 shows an SEM photograph of the morphology of the CaO prepared by spray-pyrolysis with a $Ca(NO_3)_2$ concentration of 10 wt% with the additional PS mass ratio varied between 0, 25, and 75 wt%. In general, the obtained CaO particles had an almost spherical morphology. The incomplete spherical shape is due to the rapid change in temperature of the droplets, resulting in a high evaporation rate. As a consequence, the precipitation of the materials in the droplets worsens, resulting in an incomplete spherical morphology, especially of small droplets. While the evaporation rate is higher than the diffusion rate of the particles in the solvent, during the drying process the droplet-to-particle formation only produces shell formation. Finally, during pyrolysis, the particles are broken and crushed [26]. On the other hand, the CaO powder without PS addition (Figure 3(a)) had pores because of gases released during the pyrolysis process.

The pores give the CaO powder two active surface sides (inner and outer surface). Meanwhile, the addition of 25 wt% od PS produced larger pore holes (see Figure 3(b) and Table 1) than the CaO without PS addition. This is due to the decomposition of the PS itself. However, this did not occur in the CaO powder with a high concentration (75 wt% of PS/$Ca(NO_3)_3$) of PS addition (see Figure 3(c)), which only showed a hollow on the surface of the particles. Meanwhile, from the particle size measurement it can be seen that as the PS concentration increased, the particle size decreased. This is caused by the decrease of the $Ca(NO_3)_3$ concentration in the droplets while the amount of decomposed PS particles increased and thus the volume of precipitated particles

in the droplets also decreased. Based on SEM observation, the macropores of the CaO with 25% PS addition could reach a size as large as 583.26 nm.

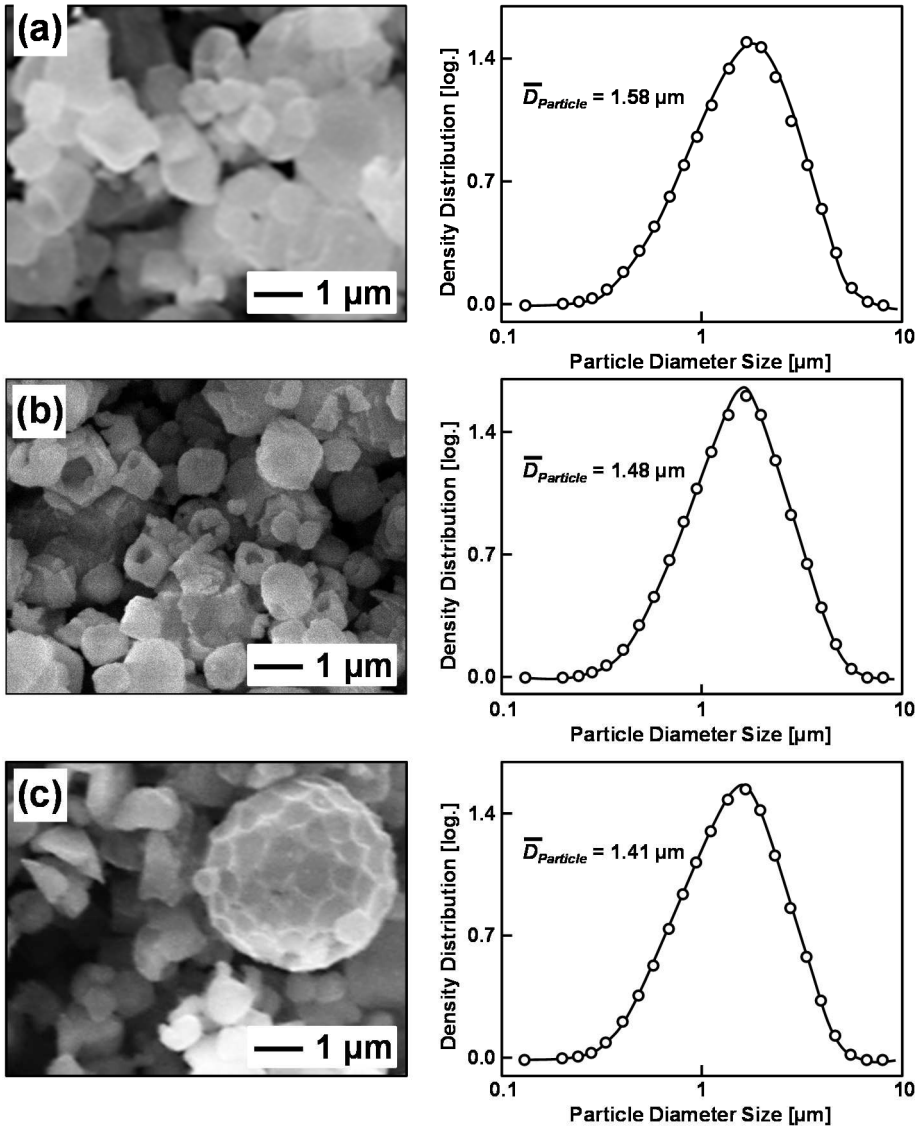

Figure 3 SEM image and particle sizes of CaO particles with (a) 0 wt%, (b) 25 wt%, and (c) 75 wt% of PS/$Ca(NO_3)_2$ mass ratio in the precursor, prepared at a synthesis temperature of 825 °C.

The mechanism of particle morphology formation affected by the PS latex concentration is shown in Figure 4. As described above, the CaO synthesized with zero PS had an incomplete spherical shape due to the high evaporation rate of the water, thus the diffusion and assembly of the precursor was poor, leading to imperfect precipitation. This also occurred in the CaO prepared with a low concentration of PS (25%). However, beside the poor assembly of the precursor in the droplets, the rapid PS decomposition also contributed to the final shape of the CaO. In a previous research, Nandiyanto *et al.* (2013) investigated the routes of particle morphology due to the PS concentration. At 20-55% PS, the particle morphology became a porous surface structure, almost identical to our result (Figure 3(b)). The differences that occurred could be due to incomplete self-assembly of the PS particles because of the high solvent evaporation rate [11]. Not only having a contribution to macropore formation, the PS decomposition may also cause mesopore formation due to its position inside the droplets. On the other hand, for a high concentration of PS addition, two particle shapes were found. A large hollow existed on the surface of the larger particles (> 1µm). The large amount of solvent in the droplets gives an opportunity for the precursor to diffuse and rearrange itself. Meanwhile, the large amount of PS decomposition breaks the smaller particles as a result of the poor assembly of the precursor, resulting in an irregular particle shape (Figure 3(c)).

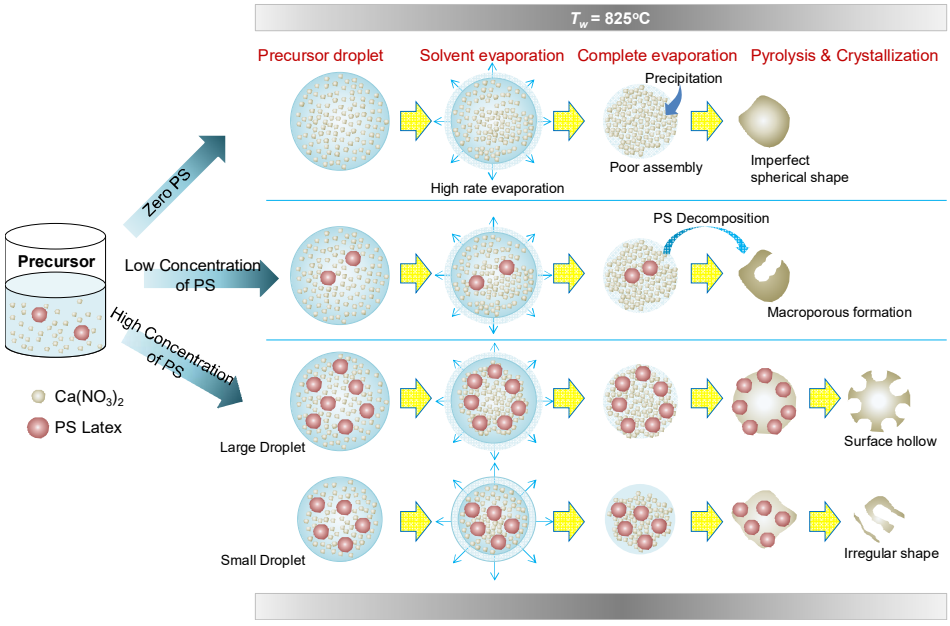

Figure 4 Illustration of CaO particle formation mechanism as a result of PS latex addition to the precursor.

Table 1 Mesoporous content of CaO particles prepared by various PS concentrations in the precursor.

Sample	PS / $Ca(NO_3)_2$ (wt%)	Pore volume (cc/g)	Pore diameter (nm)	Pore surface area (m^2/g)
1	0	0.041	3.45	8.289
2	25	0.123	5.42	12.934
3	75	0.034	3.11	6.132

In addition, the role of PS decomposition in the pyrolysis process can also be seen from the size and volume of the pores, as summarized in Table 1. From the pore measurement, it can be observed that there was a significant increase in mesopore diameter and volume from the sample without PS addition to the sample with 25 wt% PS addition. In addition, a logarithmic differential pore volume vs. pore diameter plot is depicted in Figure 5. From the figure, the significant difference between the 25% PS addition and the other CaO samples can be observed. The high volume of pores with an average diameter larger than 50 nm was demonstrated in the CaO with 25% PS addition, which could indicate the existence of macropores, which is consistent with the SEM image (Figure 2(b)). Meanwhile, the volume of the mesopore content varied for all prepared CaO samples. The pore formation was contributed by the explosion of PS as described in Figure 4. The increased pore volume and pore size also affected the surface area of the pores. The largest pore surface area was 12.934 m^2/g, found in the CaO prepared with 25 wt% PS addition.

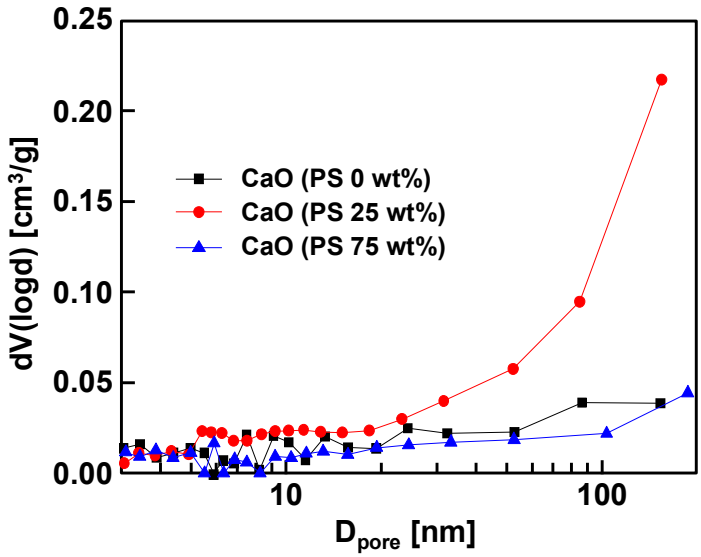

Figure 5 Logarithmic differential pore volume distribution for CaO samples prepared with different PS latex concentrations.

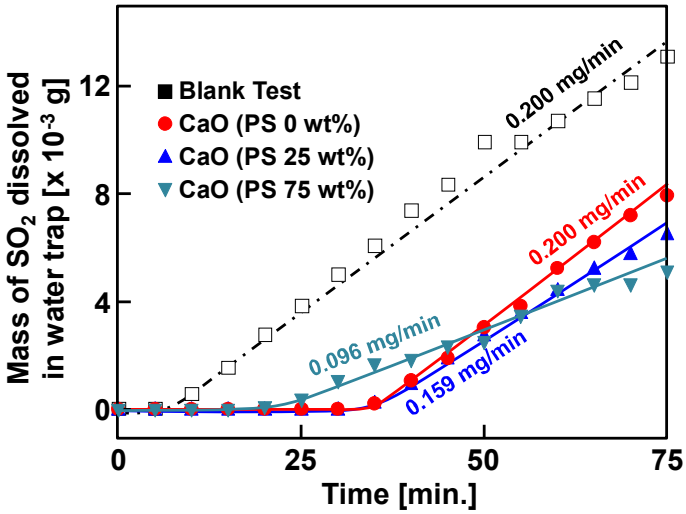

Figure 6 Profile of SO_2 dissolved in water during adsorption performance test.

Figure 6 shows the result of the SO_2 adsorption performance test, which was calculated based on the amount of SO_2 dissolved in water by pH evaluation. The low pH level of the water showed an excess of H^+ due to the formation of weak H^+ and HSO_3^- electrolytes as a result of SO_2 dissolution in water with the acid dissociation constant $k_a = 1.3 \times 10^{-2}$ at 291 K [17]. Based on the test result (Figure 6), the blank test (black-square symbol) shows linear SO_2 accumulation, which indicates a constant amount of dissolved SO_2 between two time points at a rate of 0.2 mg/min by linear fitting. This rate was utilized to approximate the amount of SO_2 captured in the CaO. Herein, the effective retention of SO_2 is defined as the amount of SO_2 that is totally captured in CaO. This is indicated by the constant level of pH even under SO_2 flow in N_2 gas as the carrier, until the point where pH starts to decrease. Referring to this definition, the effective retention capacity of CaO can be calculated as 3.32 mg, 3.32 mg, and 1.83 mg of SO_2 per 1 g of sorbent for 0, 25, and 75 % PS addition, respectively. In addition, the different rates of dissolved SO_2 from the prepared CaO could also be observed. The CaO prepared with 0% PS addition showed the same SO_2 dissolution rate as the blank test. However, the CaO prepared with 25 and 75% PS-addition showed a lower rate, i.e. 0.159 and 0.092 mg/min, respectively. The lower rate of uncaptured SO_2 compared to the blank test, indicates that the reaction between CaO and SO_2 was still occurring in the reactor. This phenomenon may be related to the formed pore size, pore volume and pore surface area. Comparing the CaO prepared with 0% and 25% PS addition, even though they have a similar effective capacitance, 3.32 mg SO_2/g sorbent, the uncaptured SO_2 rate for 25% PS addition was lower than for 0% PS addition. This phenomenon means that the capturing process of SO_2 was still occurring in

the 25% PS addition sample. On the other hand, compared to the 75% PS addition, which had the smallest pore size, pore volume, and pore surface area, the samples demonstrated the lowest retention capacitance, which shows consistency between the pore content and the adsorption ability. However, this performance test was only a simple approximation in order to observe whether the modification of CaO's surface could work properly or not. Furthermore, to get the definitive value of the retention capacity, a standard test should be considered.

Table 2 SO_2 adsorption performance test result of CaO particles.

Sample	PS / $Ca(NO_3)_2$ (wt%)	Effective SO_2 retention (mg/g CaO)	Flow rate of uncaptured SO_2 (mg/min)
1	0	3.32	0.200
2	25	3.32	0.159
3	75	1.83	0.092

Moreover, to confirm the existence of the reaction between CaO and SO_2, FTIR characterization was conducted on the powder after the adsorption test (Figure 7). Several new peaks were observed in all the post-test CaO samples, among others, two peaks around 600-700 cm^{-1}, sharp and broad peaks at 800-1000 cm^{-1}, and peaks at 1000-1200 cm^{-1}. The sharp peak around wavenumber 650 cm^{-1} and the broad peak around 800-1000 cm^{-1} correspond to the presence of (SO_3^{2-}) vibration due to the formation of $CaSO_3$ [3,26,27]. The appearance of a peak around 670 cm^{-1} indicates Ca-S bonding [3] and the peak at 1000-1200 cm^{-1} shows the presence of (SO_4^{2-}) vibration as the appearance of $CaSO_4$ [3,26,27] .

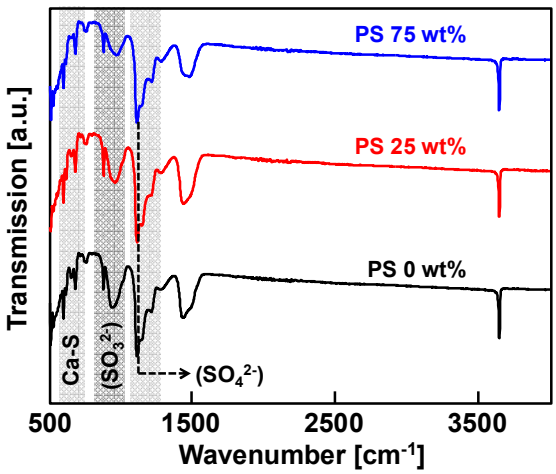

Figure 7 FTIR of CaO powder after adsorption test.

Numerous studies have been conducted to investigate the reaction of SO_2 in CaO sorbent; a simple rule of reaction between SO_2 and CaO was reported. When there is insufficient oxygen in the system, the reaction between CaO and SO_2 leads to the formation of $CaSO_3$ [28]. Furthermore, the resulting fraction of CaS and $CaSO_4$ may be due to gradual oxidation or a disproportionate amount of $CaSO_3$ [27,28]. In contrast, another work showed that the formation of $CaSO_4$ could be the direct product of the reaction between CaO and SO_2 in the temperature range of 300-600 °C [29]. On the other hand, the $CaCO_3$ fraction that occurs in the samples may contribute to the reaction during sulfation. Below the decomposition temperature, $CaCO_3$ can react directly with SO_2 to form $CaSO_3$ through the following mechanism: $CaCO_3 + SO_2 \rightarrow CaSO_3 + CO_2$ [30-32]. Moreover, under sufficient oxygen, $CaSO_3$ can be oxidized to form $CaSO_4$ [32].

4 Conclusion

In this work, the effect of PS decomposition on the formation of pores on CaO particles prepared using spray-pyrolysis was studied. The CaO particles were used as an SO_2 sorbent. BJH characterization showed that PS addition promotes the modification of the pore content in the particles. The size and volume of the pores increased with a small amount of PS addition (25 wt%), while a decrease in the total volume of pores was observed at a large amount of PS addition (75 wt%), i.e. 5.42 and 3.11 nm, respectively. The formation of pore surface was proportional to pore size and pore volume. From the SEM images, it could be seen that CaO particles without PS addition also had pores, which became larger at 25 wt% PS addition, while a hollow on the surface of the particles was observed at 75 wt% PS addition. The SO_2 adsorption performance test showed a proportional relation between the size and volume of the pores to the effective retention of SO_2. CaO particles prepared with 25 wt% PS addition gave the best performance, having a high capacity and a low rate of uncaptured SO_2 compared with the CaO prepared with 0 and 75 wt% PS addition.

Acknowledgments

The authors gratefully acknowledge the financial support from the Korea Institute of Industrial Technology (KITECH).

References

[1] Muñoz-Guillena, M.J., Linares-Solano, A. & Salinas-Martínez de Lecea, C., *High Temperature SO_2 Retention by CaO*, Appl. Surf. Sci., **99**(2), pp. 111-117, 1996.

[2] Shih, S-M., Lai, J-C. & Yang, C-H, *Kinetics of the Reaction of Dense CaO Particles with SO_2*, Ind. Eng. Chem. Res., **50**(22) pp. 12409-12420, Nov. 2011.

[3] Shuqin,W., Yi, Z., Peipei, Z. & Yandong, L, *Study of the Sulfation Kinetics between SO_2 and CaO Catalyzed by TiO_2 Nano-particles*, Chem. Eng. Res. Des, **89**(70), pp. 1061-1066, 2011.

[4] Czyżewski, A., Kapica, J., Moszyński, D., Pietrzak, R. & Przepiórski, J, *On Competitive Uptake of SO_2 and CO_2 from Air by Porous Carbon Containing CaO and MgO*, Chem. Eng. J, **226**, pp. 348-356, 2013.

[5] Shin, H-G., Kim, H., Kim, Y-N. & Lee, H-S., *Preparation and Characterization of High Surface Area Calcium Hydroxide Sorbent for SO_2 Removal*, Curr. Appl. Phys., **9**(3), Supplement, pp. S276-S279, 2009.

[6] Radfarnia, H.R. & Sayari, A., *A Highly Efficient CaO-based CO_2 Sorbent Prepared by a Citrate-assisted Sol–gel Technique*, Chem. Eng. J., **62**, pp. 913-920, 2015.

[7] Mirghiasi, Z., Bakhtiari, F., Darezereshki, E. & Esmaeilzadeh, E., *Preparation and Characterization of CaO Nanoparticles from $Ca(OH)_2$ by Direct Thermal Decomposition Method*, J. Ind. Eng. Chem., **20**(1), pp. 113-117, 2014.

[8] Sayyah, M., Abbasi, E., Lu, Y., Abbasian, J. & Suslick, K.S, Composite *CaO-Based CO_2 Sorbents Synthesized by Ultrasonic Spray Pyrolysis: Experimental Results and Modeling*, Energy & Fuels, **29**(7), pp. 4447-4452, Jul. 2015.

[9] Liu, W., Yin, J., Qin, C., Feng, B. & Xu, M., *Synthesis of CaO-Based Sorbents for CO_2 Capture by a Spray-Drying Technique*, Environ. Sci. Technol., **46**(20), pp. 11267-11272, Oct. 2012.

[10] Santos, E.T., Alfonsín, C., Chambel, A.J.S., Fernandes, A., Soares Dias, A.P., Pinheiro, C.I.C. & Ribeiroa, M.F., *Investigation of a Stable Synthetic Sol-gel CaO Sorbent for CO_2 Capture*, Fuel, **94**, pp. 624-628, 2012.

[11] Nandiyanto, A.B.D., Arutanti, O., Ogi, T., Iskandar, F., Kim, T.O. & Okuyama, K., *Synthesis of Spherical Macroporous WO_3 Particles and Their High Photocatalytic Performance*, Chem. Eng. Sci., **101**, pp. 523-532, 2013.

[12] Nandiyanto, A.B.D. & Okuyama, K., *Progress in Developing Spray-drying Methods for the Production of Controlled Morphology Particles: From the Nanometer to Submicrometer Size Ranges*, Adv. Powder Technol, **22**(1), pp. 1-19, 2011.

[13] Nandiyanto, A.B.D., Suhendi, A., Ogi, T., Iwaki, T. & Okuyama, K., *Synthesis of Additive-free Cationic Polystyrene Particles with Controllable Size for Hollow Template Applications*, Colloids Surfaces A Physicochem. Eng. Asp., **396**, pp. 96-105, 2012.

[14] Iskandar, F., Nandiyanto, A.B.D., Widiyastuti, W., Young, L.S., Okuyama, K. & Gradon, L., *Production of Morphology-controllable Porous Hyaluronic Acid Particles Using a Spray-drying Method*, Acta Biomater, **5**(4), pp. 1027-1034, 2009.

[15] Iskandar. F., Nandiyanto, A.B.D., Yun, K.M., Hogan, C.J., Okuyama, K. & Biswas, P., *Enhanced Photocatalytic Performance of Brookite TiO_2 Macroporous Particles Prepared by Spray Drying with Colloidal Templating*, Adv. Mater., **19**(10), pp. 1408-1412, 2007.

[16] Nandiyanto, A.B.D., Kim, S-G., Iskandar, F. & Okuyama, K, *Synthesis of Spherical Mesoporous Silica Nanoparticles with Nanometer-size Controllable Pores and Outer Diameters*, Microporous Mesoporous Mater., **120**(3), pp. 447-453, 2009.

[17] Yang, Z., Zhang, Y., Zhang, Q., Pei, T. & Meng, Z., *Effect of HCl on Spectral Properties of Sulfur Dioxide and its Derivatives Dissolved in Water*, Procedia Environ. Sci., **18**, pp. 92-99, 2013.

[18] Zaki, M.I., Knözinger, Tesche, H.B. & Mekhemer, G.A.H., *Influence of Phosphonation and Phosphation on Surface Acid-base and Morphological Properties of CaO as Investigated by In Situ FTIR Spectroscopy and Electron Microscopy*, J. Colloid Interface Sci, **303**(1), pp. 9-17, 2006.

[19] McDevitt, N.T. & Baun, W.L., *Infrared Absorption Study of Metal Oxides in the Low Frequency Region (700-240 cm^{-1}),* Spectrochim. Acta, **20**(5), pp. 799-808, 1964.

[20] Lutz, H.D., Eckers, W., Schneider, G. & Haeuseler, H., *Raman and Infrared Spectra of Barium and Strontium Hydroxides and Hydroxide Hydrates*, Spectrochim. Acta Part A Mol. Spectrosc, **37**(7), pp. 561-567, 1981.

[21] Arnold, T., Rozario-Ranasinghe, M. & Youtcheff, J., *Determination of Lime in Hot-Mix Asphalt*, Transp. Res. Rec. J. Transp. Res. Board, 1962, pp. 113-120, 2006.

[22] Sayyah, M., Ito, B.R., Rostam-Abadi, Lu, M.Y. & Suslick, K.S., *CaO-based Sorbents for CO_2 Capture Prepared by Ultrasonic Spray Pyrolysis*, RSC Adv., **3**(43), pp. 19872-19875, 2013.

[23] Antzara, A., Heracleous, E. & Lemonidou, A. A., *Improving the stability of synthetic CaO-based CO_2 sorbents by structural promoters*, Appl. Energy, **156**, pp. 331-343, 2015.

[24] Kukli, K., Ritala, Sajavaara, M.T., Hänninen, T. & Leskelä, M., *Atomic Layer Deposition of Calcium Oxide and Calcium Hafnium Oxide Films using Calcium Cyclopentadienyl Precursor*, Thin Solid Films, **500**(1), pp. 322-329, 2006.

[25] Scherrer, P., *Estimation of the Size and Internal Structure of Colloidal Particles by Means of Roentgen Rays*, Nach. Ges. Wiss., Gottingen, **2**, pp. 96-100, 1918.

[26] Okuyama, K. & Wuled Lenggoro, I., *Preparation of nanoparticles via spray route, Chem. Eng. Sci.*, **58**(3), pp. 537-547, 2003.
[27] Rasmussen, M.H., Wedel, S., Pedersen, K.H., Illerup, J.B. & Dam-Johansen, K., *Initial Reaction between CaO and SO_2 under Carbonating and Non-carbonating Conditions*, Chem. Eng. Sci, **134**, pp. 169-177, 2015.
[28] Ghardashkhani, S. & Cooper, D.A., *A Thermogravimetric Study of the Reaction between Sulfur Dioxide and Calcium Oxide*, Thermochim. Acta, **161**(2), pp. 327-337, 1990.
[29] Li, Y. & Sadakata, M., *Study of Gypsum Formation for Appropriate Dry Desulfurization Process of Flue Gas*, Fuel, **78**(9), pp. 1089-1095, 1999.
[30] Baltrusaitis, J., Usher, C.R. & Grassian, V.H., *Reactions of Sulfur Dioxide on Calcium Carbonate Single Crystal and Particle Surfaces at the Adsorbed Water Carbonate Interface*, Phys. Chem. Chem. Phys, **9**(23), pp. 3011-3024, 2007.
[31] Tullin, C. & Ljungström, E., *Reaction between Calcium Carbonate and Sulfur Dioxide*, Energy and Fuels, **3**(3), pp. 284-287, 1989.
[32] Van Houte, G., Rodrique, Genet, L.M. & Delmon, B., *Kinetics of the Reaction of Calcium Sulfite and Calcium Carbonate with Sulfur Dioxide and Oxygen in the Presence of Calcium Chloride*, Environ. Sci. Technol, **15**(3), pp. 327-332, 1981.